Supporting Information for

Particle Aggregation Mechanisms in Ionic Liquids

Istvan Szilagyi, Tamas Szabo, Anthony Désert, Gregor Trefalt, Tamas Oncsik, Michal Borkovec*

*Corresponding author: Phone: + 41 22 379 6405, E-mail: michal.borkovec@unige.ch

Materials. Spherical negatively charged sulphate and positively charged amidine functionalized polystyrene latex particles were purchased from Interfacial Dynamics Corporation (Portland, USA). Their size and charge are summarized in Table S1. The manufacturer further reports the density of the latex particles as 1.05 g/cm^3. The purchased aqueous stock suspensions were purified by dialysis against Milli-Q water (Millipore, Molsheim, France). Milli-Q water was used throughout. For the amidine particles, polyvinylidene difluoride membranes and for the sulphate particles cellulose ester membranes, both with a molecular mass cut-off of 300 kg/mol were used (Spectrum Rancho, Dominguez, USA). The dialysis was performed until the conductivity of the surrounding medium reached the value of Milli-Q water. The stock suspension was subsequently diluted for light scattering measurements and adjusted to pH 5.0 by HCl. The precise particle concentration was determined by static light scattering by comparing the scattered intensities with the samples of known particle concentration and with total carbon and nitrogen analysis (TOCV, Shimadzu, Japan).

The following water miscible room temperature ILs were purchased from IoLiTech GmbH (Heilbronn, Germany): 1-butyl-3-methylimidazolium tetrafluoroborate, BMIM-BF_4, 1-butyl-3-methylimidazolium dicyanamide, BMIM-$N(CN)_2$, 1-butyl-3-methylimidazolium thiocyanate, BMIM-SCN, 1-butylpyridinium tetrafluoroborate, BPY-BF_4, 1-butyl-3-methylpyridinium dicyanamide, BMPY-$N(CN)_2$, and 1-butyl-1-methylpyrrolidinium dicyanamide, BMPL-$N(CN)_2$ (Table S2). The ILs were dried under vacuum at 50°C and the final water content was determined by Karl-Fischer titration (Metrohm, Herisau, Switzerland). The water content was below 1 g/L. IL impurities originating from the synthetic procedures are given in Table S3. The dried ILs were handled in a glove box. A precipitate sometimes appeared after mixing the ILs with water, which could be easily detected by light scattering. This precipitate could be removed by leaving the sample standing overnight, and filtering with 0.2 μm syringe filter (Millipore, Molsheim, France). However, the precipitate could not be removed in BMPY-$N(CN)_2$-water mixtures at low IL-to-water ratios, and therefore the aggregation rates could not be determined under these conditions. All experiments are carried out at 25.0±0.2 °C.

Properties of ILs and their water mixtures. Density, refractive index, and viscosity of the ILs and their water mixtures were determined with standard techniques. Densities were measured with a Krüss Easy Dyne K20 tensiometer (Krüss GmbH, Hamburg, Germany) by weighing a silicon crystal cylinder immersed in the IL-water mixture. The uncertainty of the measurements was estimated to be ±0.001 g/cm^3. Data for BMIM-SCN, BMPL-$N(CN)_2$ and BPY-BF_4 were taken from literature.[1-3] The experimental data were fitted with the ideal mixing law

$$\rho = \frac{1}{(1-y)/\rho_{\mathrm{W}} + y/\rho_{\mathrm{IL}}} \tag{1}$$

where y is the mass fraction of the IL, and $\rho_{\mathrm{W}} = 0.997$ g/cm^3 is the density of water and ρ_{IL} are the densities the IL given in Table S2. The ideal mixing law is accurate within 0.7% for all IL-water mixtures studied. The data and fits are shown in Fig. S1.

Refractive index measurements were carried out with an Abbemat-WR/MW automatic multiwavelength refractometer (Anton Paar, Zofingen, Switzerland) at wavelengths of 533 nm and 632 nm, which correspond to the laser wavelength of the light scattering instruments used. The data were fitted with the ideal mixing law

$$n = n_{\mathrm{W}}(1-\phi) + n_{\mathrm{IL}}\phi \tag{2}$$

where ϕ is the volume fraction of the IL, and n_{W} and n_{IL} are the refractive indices of water and the IL, respectively. The refractive index of water is 1.334 at 533 nm and 1.331 at 632 nm, while the ones for the ILs are given in Table S2. The volume fraction was calculated assuming the mixing law eq. (1) for the density. The ideal mixing law for the refractive index is accurate within 0.4% for all IL-water mixtures studied.

Shear viscosities were measured with a Brookfield LVDV-II+ Pro C/P viscometer (Hunter and Caprez, Zumikon, Switzerland) in a cone-plate geometry with the CPE-40 cone. The data were recorded with the IL-water mixture. The shear stress always showed a linear dependence with the shear rate, indicating that the ILs are Newtonian liquids. The viscosities of the IL-water systems were fitted with a polynomial model[4]

$$\eta = \eta_{\mathrm{W}}(1-x) + \eta_{\mathrm{IL}}x + x(1-x)\sum_{i=0}^{4} a_i \left(2x-1\right)^i \tag{3}$$

where x is the mole fraction of IL, η_{W} and η_{IL} are the viscosities of water and pure IL. The viscosity of pure water is 0.890 mPas, while the ones of the ILs are given in Table S2. The fitting parameters a_i are given in Table S4. For some ILs a satisfactory fit could be achieved by setting the higher order coefficients to zero. This model describes the viscosity data within about 1%.

Light Scattering. The size and optical properties of particles were characterized by static light scattering (SLS) in both aqueous electrolyte (KCl, Acros Organics, Geel, Belgium) and IL solutions as well as in pure ILs. The intensity of the scattered light was recorded at several scattering angles with a multi-angle goniometer with 8 photomultiplier detectors (ALV/CGS-8F, Langen, Germany) equipped with a 532 nm solid-state Verdi V2 laser. The measurements in stable suspensions were performed at particle concentrations of 10 mg/L and 50 mg/L for amidine and sulphate latex, respectively. Time-resolved aggregation experiments by multi-angle SLS and DLS were carried out in 1.0 M KCl aqueous electrolyte and in BMIM-SCN solutions at an IL-to-water molar ratio of 0.09 and 0.27 for the amidine and sulphate latex particles, respectively. Particle concentrations of 1.2 and 5.0 mg/L were used for the amidine latex of 110 nm in radius in the presence of KCl and IL respectively, while 1.2 and 25.0 mg/L for sulphate latex particles of 265 nm in radius. Even for the largest particles used, sedimentation or creaming effects are negligible as could be confirmed from the constancy of

the absolute light scattering intensity in stable suspensions over 24 h. Most aggregation measurements were performed at a single scattering angle of 90° on the compact goniometer system (ALV/CGS-3, Langen, Germany). The instrument uses a He/Ne laser operating at 633 nm as a light source and an avalanche photodiode as a detector. The time-resolved DLS experiments were performed in borosilicate glass cuvettes. Cuvettes were cleaned with a hot piranha solution consisting of 30% H_2O_2 and concentrated H_2SO_4 in a volume ratio of 1:3 and rinsed extensively with water followed by drying in dust-free environment. The ILs were mixed with the appropriate amount of water. The experiments were started by adding a small amount of the aqueous particle suspension into the cuvette and mixing with a vortex stirrer. This procedure limited the lowest achievable water content to about 3 g/L. The final particle concentration was about 10 mg/L, which was adequately low to keep the aggregation in its early stages. To obtain reliable results for slow aggregating suspensions, the particle concentration was increased about 10-fold compared to the concentrations used for the other experiments. The scattering signal of the pure ILs was about 3–10 times larger than for toluene. This larger scattering intensity probably originates from the nm-scale structures that spontaneously from in the ILs. However, these scattering intensities are still about three times lower than the one of the suspensions containing nano-sized sulphate latex and at least two orders of magnitude lower than the one for the sub-micron particles. Differential sedimentation effects on the early stages of the aggregation are negligible due to the small particle polydispersity.

References

1 U. Domanska and M. Krolikowska, *J. Solut. Chem.,* 2012, **41**, 1422-1445.
2 E. J. Gonzalez, A. Dominguez and E. A. Macedo, *J. Chem. Eng. Data,* 2012, **57**, 2165-2176.
3 B. Mokhtarani, A. Sharifi, H. R. Mortaheb, M. Mirzaei, M. Mafi and F. Sadeghian, *J. Chem. Thermodyn.,* 2009, **41**, 323-329.
4 O. Redlich and A. T. Kister, *Ind. Eng. Chem.,* 1948, **40**, 345-348.
5 J. Nordstrom, L. Aguilera and A. Matic, *Langmuir,* 2012, **28**, 4080-4085.
6 J. A. Smith, O. Werzer, G. B. Webber, G. G. Warr and R. Atkin, *J. Phys. Chem. Lett.,* 2010, **1**, 64-68.
7 K. Ueno, A. Inaba, M. Kondoh and M. Watanabe, *Langmuir,* 2008, **24**, 5253-5259.
8 E. Vanecht, K. Binnemans, S. Patskovsky, M. Meunier, J. W. Seo, L. Stappers and J. Fransaer, *Phys. Chem. Chem. Phys.,* 2012, **14**, 5662-5671.

Table S1. Properties of particles used.

Latex Particles	Radius (nm)			Polydispersity (%)[d]		Surface Charge (mC/m^2)[e]
	TEM[a]	SLS[b]	DLS[c]	TEM[a]	SLS[b]	
Sulphate	265	263	278	2.0	3.8	–19
Nano-Sized Sulphate	50	56	58	7.9	7.9[f]	–17
Amidine	110	110	117	4.3	7.1	10

[a]Measured by transmission electron microscopy by the manufacturer. Measured in static[b] and dynamic[c] light scattering experiments in stable suspensions. [d]Coefficient of variation. [e]Determined from the electrophoretic mobilities with the standard electrokinetic model in aqueous KCl solutions. [f]The value was kept fixed during the fit.

Table S2. Properties of pure ILs used at 25°C.

Ionic Liquid	Molecular Mass (g/mol)	Density (g/mL)	Refractive index (at 533 nm)	Refractive index (at 633 nm)	Viscosity (mPas)
BMIM-BF_4	226.0	1.201	1.422	1.418	104.0
BMIM-SCN	197.3	1.070	1.542	1.534	56.5
BMIM-$N(CN)_2$	205.3	1.060	1.512	1.505	30.0
BMPY-$N(CN)_2$	216.3	1.054	1.540	1.532	47.5
BMPL-$N(CN)_2$	208.3	1.013	1.499	1.494	34.6
BPY-BF_4	223.0	1.208	1.447	1.441	149.7

Table S3. Impurities of the ILs used as reported by manufacturer (in mg/L).

IL	F^-	Cl^-	Br^-	Na^+	NH_4^+	MIM[a]	MPL[b]	PY[c]
BMIM-SCN	–	690	–	–	2770	9680	–	–
BMIM-$N(CN)_2$	–	9360	30	–	–	180	–	–
BMIM-BF_4	50	10	10	–	–	210	–	–
BMPY-$N(CN)_2$	–	17000	20	2960	–	–	–	7760[d]
BMPL-$N(CN)_2$	–	2870	200	–	–	–	50	–
BPY-BF_4	–	10	–	1000	–	–	–	1000

[a]1-Methylimidazole. [b]1-Methylpyrrolidine. [c]Pyridine. [d]3-Methylpyridine.

Table S4. Parameters of the polynomial model fit of the viscosity as given by eq. (3).

Parameter	BMPL-$N(CN)_2$	BMPY-$N(CN)_2$	BMIM-$N(CN)_2$	BMIM-SCN	BMIM-BF_4	BPY-BF_4
a_0	4.75	–13.2	–4.88	–41.1	–149	–239
a_1	5.71	10.6	4.18	8.80	89.6	171
a_2	–14.3	–5.10	–6.10	–2.44	–14.6	–98.2
a_3	–6.53	–11.4	1.07	0	–27.6	34.9
a_4	0	0	0	0	–17.4	0

Table S5. Critical coagulation concentrations (CCC) for latex particles in IL-water mixtures.

	Amidine Latex		Sulphate Latex	
	CCC-W[a]	CCC-IL[b]	CCC-W[a]	CCC-IL[b]
KCl	0.19±0.01	–[c]	0.30±0.01	–[c]
BMIM-BF_4	0.10±0.01	0.8±0.6	0.050±0.005	0.9±0.6
BMIM-SCN	0.03±0.01	1.8±0.1	0.11±0.002	13±1
BMIM-$N(CN)_2$	0.050±0.005	3.2±0.2	0.093±0.008	5.6±0.6
BMPY-$N(CN)_2$	–[d]	6.7±0.3	–[d]	3.2±0.1
BMPL-$N(CN)_2$	0.060±0.005	2.6±0.2	0.057±0.003	10±0.8
BPY-BF_4	0.060±0.007	0.9±0.6	0.055±0.004	0.8±0.6

[a]Concentration of the ILs in mol/L. [b]Concentration of water in mol/L. [c]There is no such CCC since the solubility limit is reached beforehand. [d]The CCC could not be determined due to formation of precipitates.

Table S6. Properties of the previously published particle suspensions in ILs shown in Fig. 1.

Particle type	Mean Particle Radius (nm)	IL	Time (s)[a]	Particle Concentration (m^{-3})	Reference
Silica[b]	6.0	BMIM-BF_4	7.2×10^4	1.6×10^{22}	Nordström et al.[5]
Silica	580	EA-NO_3[c]	7.2×10^4	7.2×10^{18}	Smith et al.[6]
Silica[d]	62	BMIM-PF_6	4.3×10^4	1.9×10^{22}	Ueno et al.[7]
Gold	3.0	BMIM-$N(CN)_2$	1.2×10^6	1.2×10^{20}	Vanecht et al.[8]

[a]Time over which the suspension was reported to be stable. [b]Fumed silica particle was used and the system contained $LiBF_4$ as well. [c]Ethylammonium nitrate. [d]Silica particles with grafted with poly(methyl methacrylate) on the surface.

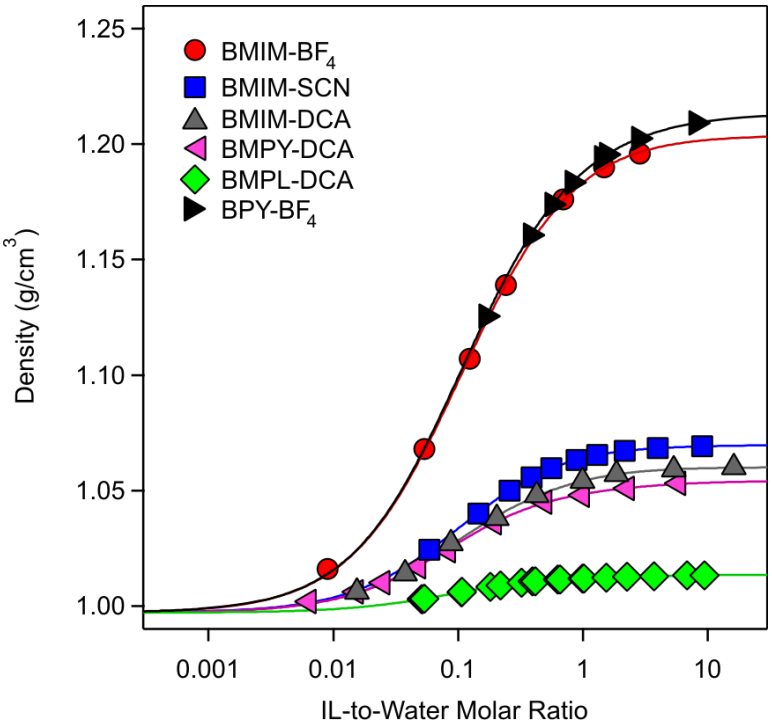

Figure S1. Densities versus the IL-to-water molar ratios. The symbols are experimental data and the lines correspond to the ideal mixing law eq. (1).

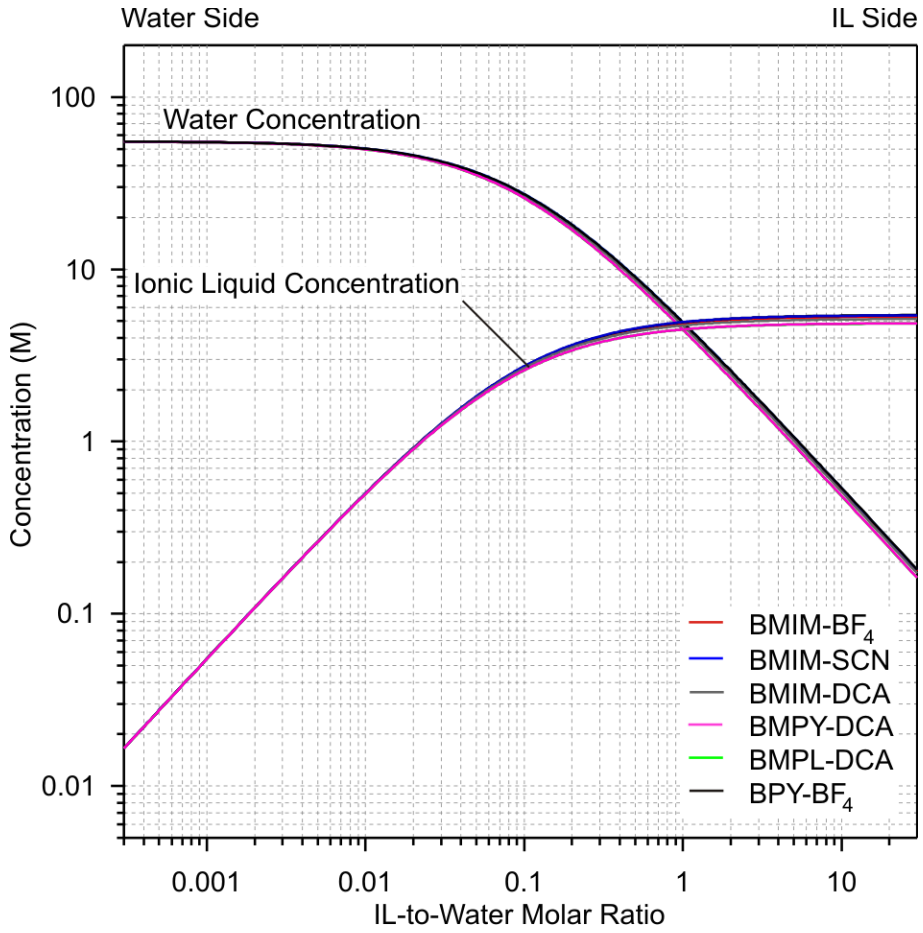

Figure S2. Molar concentrations in IL-water mixtures as a function of the IL-to-water molar ratios. The water and IL molar concentrations are shown. The different lines indicate the different ILs used in the present study.

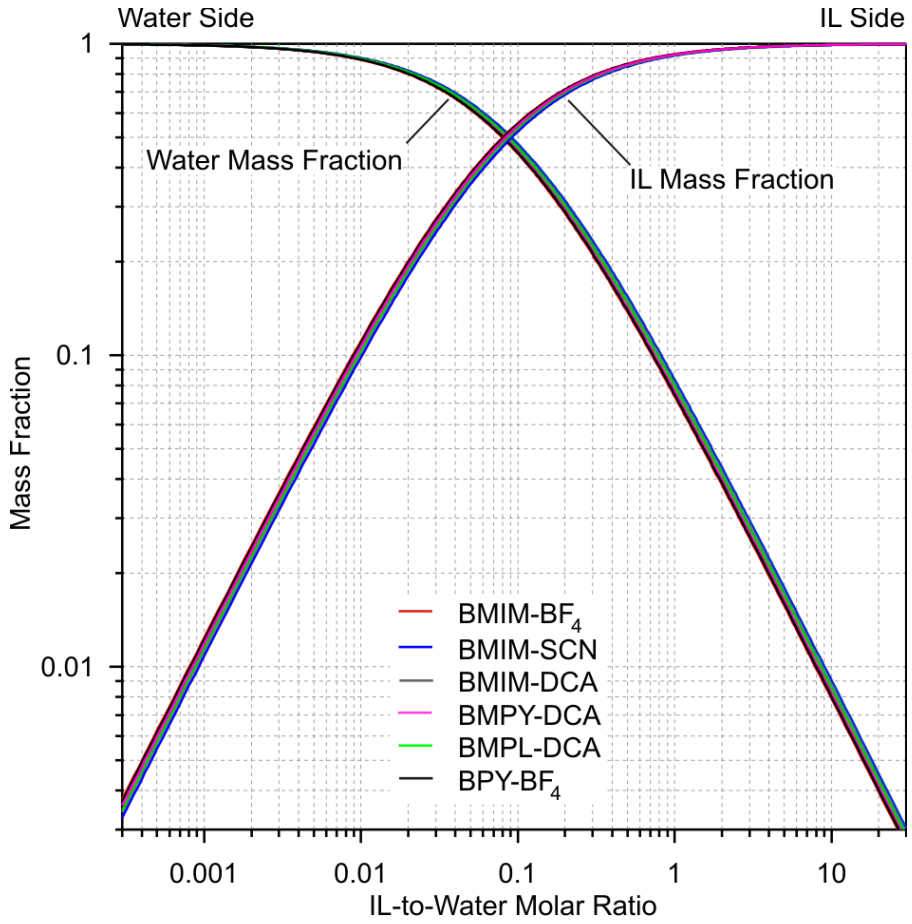

Figure S3. Mass fractions in IL-water mixtures as a function of the IL-to-water molar ratios. The water and IL mass fractions are shown. The different lines indicate the different ILs used in the present study.

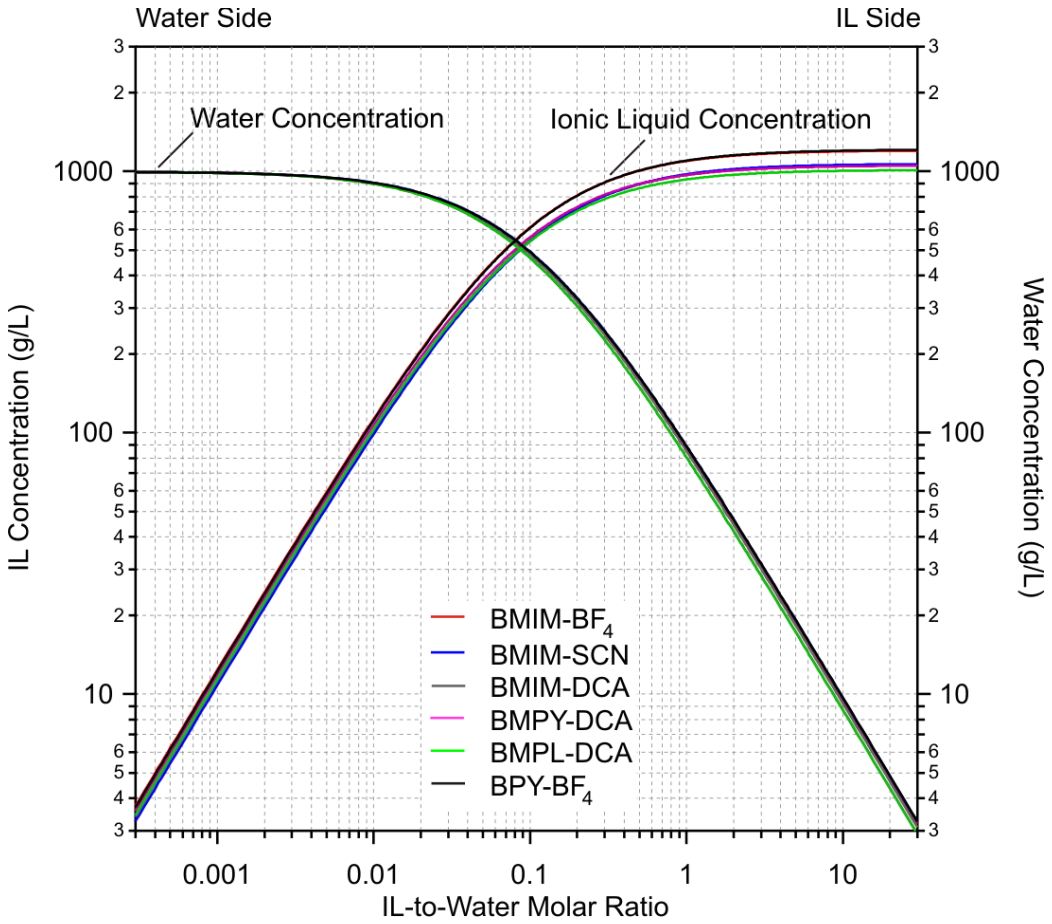

Figure S4. Mass concentrations in IL-water mixtures as a function of the IL-to-water molar ratios. The water and IL mass concentrations are shown. The different lines indicate the different ILs used in the present study.